

## Second-Harmonic Diffraction from Periodically Modulated Molecular Monolayers

T. F. Heinz and T. Suzuki\*

IBM Research Division, T. J. Watson Research Center,  
Yorktown Heights, NY 10598

### ABSTRACT

The surface-specific process of optical second-harmonic generation has been applied to investigate adsorbed molecular monolayers exhibiting a periodic modulation across the surface. In addition to the usual reflected second-harmonic signals, these spatially modulated monolayers are found to give rise to several orders of diffracted second-harmonic radiation. An analysis is presented relating the characteristics of the second-harmonic diffraction pattern to the spatial properties of the modulated adlayer. In this study, gratings in the adsorbate density of dye molecules adsorbed on insulating substrates were formed by photo-desorption in the field of two interfering laser beams. From the second-harmonic diffraction data, adsorbate density profiles have been inferred. These results can be explained by a model for the formation of the molecular gratings based on a thermal desorption mechanism.

### 1. INTRODUCTION

Techniques based on induced gratings have proved to be very powerful tools in examining a number of important properties of bulk materials. In these methods, two interfering laser beams illuminate the system under study, leading to the formation of a modulation in the optical constants of the material. The presence of this grating is sensed by means of diffracting another laser beam from it. The strength of the induced modulation and its temporal character, as well as its dependence on the wavelength of the radiation producing the grating, can yield a wide variety of information about the material.<sup>1</sup> The scheme has, for example, been applied to investigate the diffusion of photo-excited carriers in semiconductors.<sup>2</sup> This is accomplished by observing the decay in the diffraction efficiency as an initially imposed spatial modulation in the carrier density disappears through diffusion.

The possibility of carrying out analogous measurements for surface and interfaces rather than for bulk materials is an intriguing one. The nonlinear optical process of second-harmonic generation (SHG) provides a natural approach for obtaining the necessary discrimination to detect a grating in the surface layer of centrosymmetric medium (or at the interface of two centrosymmetric media). This surface specificity, which arises from the fact that second-order nonlinear optical effects are forbidden (within the electric-dipole approximation) in the bulk of centrosymmetric media, has already been exploited in a wide variety of investigations of the nature of homogeneous surfaces.<sup>3</sup> Several independent studies have recently been conducted involving the production of diffracted second-harmonic (SH) radiation from a surface with spatially modulated properties.<sup>4-6</sup> Reider *et al.*<sup>4</sup> have reported the observation of first-order diffraction of SH radiation from a spatially modulated molecular monolayer produced by a direct writing scheme. In this work, it was demonstrated that it is possible to obtain monolayer sensitivity even for surfaces of non-centrosymmetric bulk media by examining diffracted SH radiation. Zhu *et al.*<sup>5</sup> have utilized SH diffraction into the first-order to determine surface diffusion rates of CO adsorbed on a Ni(111) surface. These measurements were performed monitoring the decay in the SH diffraction efficiency as a function of elapsed time subsequent to the formation of a modulated adsorbate density profile by laser-induced desorption. In our studies, we have produced permanent gratings of monolayer thickness by exposing a surface covered by an adsorbed monolayer of large organic molecules to the field of two intense interfering laser beams. As we report here, these monolayer gratings give rise to easily observable SH radiation in several diffracted orders. We discuss, further, how the measured diffraction patterns can be related to the spatial properties of the grating. This leads to a simple model for the formation of the molecular grating by laser-induced desorption based on a thermal mechanism.

\* Permanent address: RIKEN, The Institute of Physical and Chemical Research, Wako, Saitama, Japan

## 2. SECOND-HARMONIC DIFFRACTION: GENERAL CONSIDERATIONS

For a homogeneous centrosymmetric medium, we can describe the second-harmonic response of the surface by a nonlinear susceptibility tensor  $\chi_s^{(2)}$  relating the nonlinear source polarization per unit area to the pump electric field. If spatial variation is present across the surface, it will be reflected in the nonlinear susceptibility  $\chi_s^{(2)} = \chi_s^{(2)}(x,y)$ , where  $x$  and  $y$  are coordinates in the surface. Since we are interested in the case of a periodic modulation, let us introduce a wave vector  $k_g$  to characterize a surface grating of period  $l_g = 2\pi/k_g$ . The surface nonlinear susceptibility can then be written in the form of a Fourier series as

$$[1] \quad \chi_s^{(2)}(\mathbf{x}) = \sum_{n=-\infty}^{\infty} \chi_s^{(2)}(n) e^{in\mathbf{k}_g \cdot \mathbf{x}}.$$

Under excitation at frequency  $\omega$  by a plane wave with field strength  $\mathbf{E}_g^\omega$  at the surface, a nonlinear polarization

$$[2] \quad \mathbf{P}_s^{2\omega}(\mathbf{x}) = \sum_{n=-\infty}^{\infty} \chi_s^{(2)}(n) : \mathbf{E}_g^\omega \mathbf{E}_g^\omega e^{i(2\mathbf{k}_g + n\mathbf{k}_g) \cdot \mathbf{x}}$$

will appear. Here  $k_\parallel$  denotes the component of the wave vector of the pump field  $\mathbf{k}^\omega$  lying in the plane of the surface.

From Eq. [2], we see that radiation at the second-harmonic frequency is allowed in directions defined by  $\mathbf{k}_\parallel^{2\omega}(n) = 2\mathbf{k}_\parallel^\omega + n\mathbf{k}_g$ . For  $n = 0$ , this just corresponds to the usual transmitted and reflected beams. For dispersionless media, these waves travel along the directions of the transmitted and reflected pump beams. The diffracted radiation emerges in directions defined by the wave vector matching relation for  $n = \pm 1, \pm 2, \pm 3, \dots$ . This type of diffraction process has been reported previously by Wokaun *et al.*<sup>7</sup> in studies of SH generation from an array of metal microstructures. For comparison with experiment, we consider in somewhat more detail the case of a grating with grooves running perpendicular to the plane of incidence of the pump radiation. The diffracted SH beams will then lie in the plane of incidence. In our measurements the diffracted beams are detected by rotating the sample about an axis perpendicular to the plane of incidence. The directions of the incident pump and detected SH beams are held fixed at an angle  $2\theta_0$  with respect to one another. The criterion for observing the  $n$ th-order diffracted SH beam will be met for pump radiation with an angle of incidence of

$$[3] \quad \theta(n) = \theta_0 + \sin^{-1}[n(k_g/k^\omega)/(4 \cos \theta_0)].$$

The surface nonlinear susceptibility  $\chi_s^{(2)}$  is sensitive to many aspects of the properties of the surface. Hence, one can conceive of a wide variety of possible surface gratings leading to nonlinear diffraction. For example, the orientation of molecular adsorbates will generally strongly influence the nonlinear susceptibility, making possible diffraction from an orientational grating. By the same token, a periodic modulation in electronic or vibrational excitation (or in the temperature of a thermalized system) should give rise to nonlinear scattering. In this paper, we restrict our attention to the simple case of a grating in the density of an adsorbed species. In accordance with the experiment, we attribute all of the nonlinear response to the adsorbed layer. Then under the neglect of local field corrections for non-interacting molecules, we can write the spatially varying nonlinear susceptibility in terms of the spatially varying adsorbate density as  $N_s(x,y)$ :

$$[4] \quad \chi_s^{(2)}(x,y) = \chi_{s,0}^{(2)} [N_s(x,y)/N_{s,0}].$$

In this equation,  $\chi_{s,0}^{(2)}$  represents the nonlinear susceptibility of a spatially homogeneous surface with an adsorbate density  $N_{s,0}$ ; and  $x$  and  $y$  are coordinates in the plane of the surface. For a periodically modulated adsorbate density,

$$[5] \quad N_s(x,y) = \sum_{n=-\infty}^{\infty} N_s(n) e^{in\mathbf{k}_g \cdot \mathbf{x}},$$

each Fourier component of the surface nonlinear susceptibility is proportional to the corresponding component of the expansion of the adsorbate density. By considering the radiation arising from the nonlinear polarization of Eq. [2], one can then relate the diffracted SH field of order  $n$  to  $N_s(n)$ . For the case of diffraction of the SH beams into a narrow range of angles, one has simply<sup>6</sup>

$$[6] \quad N_s(n)/N_{s,0} = E^{2\omega}(n)/E_0^{2\omega},$$

where the  $n$ th order SH fields,  $E^{2\omega}(n)$ , are assumed to be measured with a given combination of pump and detected polarizations. Eq. [6] gives us, within the approximations of the analysis, a quantitative relation between the SH diffraction and the surface density profile.

### 3. EXPERIMENT

The monolayer gratings investigated in these studies consisted of Rhodamine 6G dye molecules on fused silica and sapphire substrates. The homogeneous films were prepared on substrates cleaned in a succession of solvents. The dye molecules were deposited by spinning a substrate covered by a thin layer of dye molecules in an ethanol solution at high speed, as in Ref. 8. By varying the concentration of the dye molecules in the solution, we could control the adsorbate density on the surface. Measurements of the SH response indicated an increasing signal up to a concentration of  $\sim 10^{-4}$  M/l. Beyond that point, the SH signal reached a plateau and then gradually declined. The increasing SH response is associated with the build up of the first monolayer of the adsorbed species; the subsequent decrease is presumed to arise from multilayer formation. The results reported here were obtained by the spinning technique with a dye concentration of  $3 \times 10^{-4}$  M/l. This is expected to yield approximately 1 monolayer coverage of the adsorbate. From linear optical measurements of the absorption at the peak of the  $S_1 \leftarrow S_0$  transition, an average surface density of  $\sim 7 \times 10^{13}$  cm $^{-2}$  was inferred for the homogeneous films.

The grating in the adsorbed dye layer was formed by exposing the sample to the frequency-doubled output of a Q-switched Nd-doped yttrium aluminum garnet (Nd:YAG) laser. The radiation consisted of pulses of 6 nsec (FWHM) duration at a wavelength of 532 nm. The laser radiation was split into two beams of equal intensity, which were recombined on the surface of the sample at angles of  $\pm 2.0^\circ$  with respect to the surface normal. Based on the angle between the two interfering laser beams, the period of the molecular grating produced by the process of laser-induced desorption is  $l_g = 7.6\mu\text{m}$ . In the experiment, each grating was formed by a single laser shot. Key to obtaining a well-defined surface structure was meeting the condition that the two interfering beams be coherent with respect to one another; this necessitated matching the lengths of each arm in the optical path to within a fraction of a centimeter. The molecular gratings were found to be stable under ambient conditions during the course of the experiments. They showed no obvious sign of degradation, either from desorption, diffusion, or surface chemical reactions.

For measurements of SHG from the modulated molecular films, we employed nanosecond pulsed laser radiation at 690 nm. The wavelength of the pump beam was selected to take advantage of a resonant enhancement of the SHG arising from the  $S_2 \leftarrow S_0$  transition at the SH frequency.<sup>8</sup> It should be noted that the adsorbed molecules did not exhibit any appreciable absorption at the fundamental frequency of the pump beam, so laser-induced processes are not anticipated at moderate intensities. The laser was lightly focussed on the sample so as to lie well within the area irradiated by the crossed beams, thereby probing a uniform region of the molecular grating. The SH radiation was detected with a photomultiplier and gated electronics after radiation at the SH frequency had been isolated using color filters and a monochromator. The molecular grating was aligned with its grooves perpendicular to the plane of incidence of the pump light. The different diffracted SH beams then all emerged in the plane of incidence. Rather than rotating the detection system, a fixed detection geometry was employed and the sample was rotated through an axis perpendicular to the plane of incidence to measure the different diffracted beams. The detection system was arranged to accept light propagating at  $90^\circ$  with respect to the pump beam. Thus, the specular reflection ( $n = 0$  diffracted beam) occurred with the sample aligned to make an angle of incidence of  $\theta_0 = 45^\circ$ ; the other diffracted beams were observed when the sample was rotated in either direction away from this position. Measurement of the SH diffraction were performed with various combinations of pump and detected polarizations.

#### 4. SH DIFFRACTION FROM MONOLAYER GRATINGS

Results from SH diffraction measurements of two molecular gratings formed on fused silica substrates are shown in Fig. 1. In the upper panel, the second harmonic intensity for the homogeneous film is indicated by a dotted line. As we would anticipate, only the reflected beam at an angle of incidence of  $45^\circ$  is observed. The solid curve in Fig. 1(a) corresponds to diffraction from a relatively weak grating produced with a average laser fluence at the surface of  $1.1 \text{ J/cm}^2$ . We note that the strength of the reflected SH signal drops, in accordance with the decrease in the average density of the adsorbed species. First-order diffracted SH radiation is also observed. The lower panel displays data from a more strongly modulated grating, which was formed with a desorbing laser fluence of  $1.6 \text{ J/cm}^2$  at the surface. In addition to the sharp decrease in the strength of the SH reflection, we now observe diffracted radiation of orders  $n = 1$  and  $n = 2$ . The arrows in the Figure are the positions of the diffracted peaks calculated from Eq. [3] with  $\theta_0 = 45^\circ$ . The same data for diffraction from the weak and strong gratings are presented in Fig. 2 in terms of the SH field strength in order to accentuate the presence of the diffracted beams. The data in Figs. 1 and 2, were collected using p-polarized pump and detected radiation. Combinations of polarizations compatible with a symmetry-allowed SHG process from an isotropic surface were investigated. The ratio of diffracted intensities was always the same within experimental accuracy, in accordance with our picture of a molecular grating in the density (not, for example, the orientation) of the adsorbed species.

We have also produced gratings of Rhodamine 6G molecules on sapphire substrates. The degree of modulation obtainable was always very modest. Figure 3 illustrates this point with a comparison of a grating on a sapphire substrate [Fig.3(a)] and one on a fused silica substrate [Fig.3(b)]. The two gratings were produced with a comparable laser fluence of  $1.8 \text{ J/cm}^2$  at the surface. At this higher fluence, diffraction up to third (or, perhaps, fourth) order is observed for the grating on the fused silica substrate. Only weak first-order diffraction is present for the molecular grating formed on the sapphire substrate. We present a qualitative explanation for the different behaviors below.

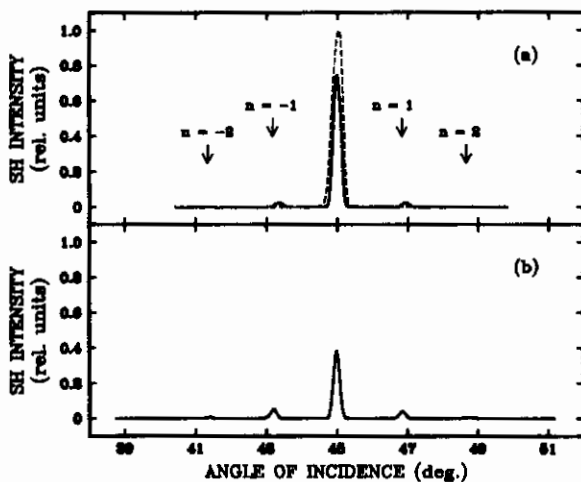


Fig. 1. Diffracted SH intensity from a monolayer of Rhodamine 6G molecules adsorbed on a fused silica substrate as a function of sample rotation. (a) shows the results from the monolayer before (dashed curve) and after (solid curve) the formation of a grating with a laser fluence of  $1.1 \text{ J/cm}^2$ ; (b) corresponds to a grating produced with a laser fluence of  $1.6 \text{ J/cm}^2$ .

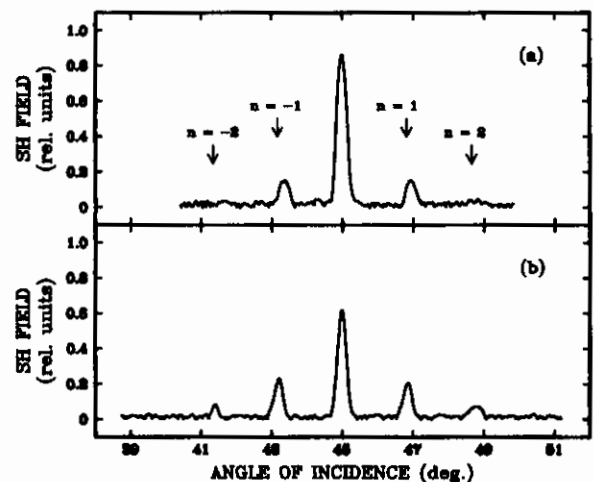


Fig. 2. Diffracted SH field strengths for the diffraction patterns of Fig. 1.

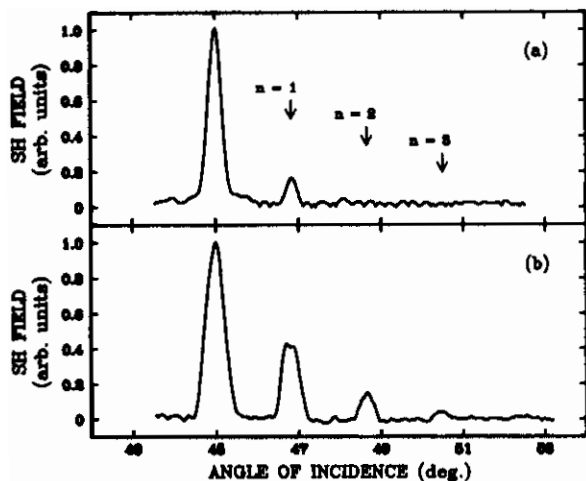


Fig. 3. Diffracted SH field strengths for monolayer gratings of Rhodamine 6G molecules adsorbed on (a) sapphire and (b) fused silica substrates. In both cases, the fluence of the desorbing laser was approximately  $1.8 \text{ J/cm}^2$ .

## 5. ANALYSIS AND DISCUSSION

One of the interesting questions is that of reconstructing the average adsorbate density profile from the data on SH diffraction. Within the approximations of our treatment, application of Eq. [6] provides the means. We are, however, still missing one necessary piece of information: we do not know the relative signs of the different diffracted SH fields, only the relative field strengths. Methods have been developed to determine the phase of SH radiation<sup>9</sup>, but their application for the case of diffracted radiation is not trivial. For our present work, we have only a few signs to determine. By applying the constraint that the density profile must stay between 0 and  $N_{s,0}$  (the surface density before formation of the grating), we can establish the required sign relations. The sign of  $N_s(0)$ , representing the average adsorbate density, must clearly be positive. As for  $N_s(1)$ , we can arbitrarily assume its sign to be positive: the choice of a negative sign at this point would only produce a shift in the adsorbate profile. Then from examining inferred density profiles for several grating structures, we find that  $N_s(2)$  should be taken as negative and  $N_s(3)$  as positive.

The solid curves in Fig. 4 represent the adsorbate density profiles inferred from the data in Figs. 1 and 2 with the signs for  $N_s(n)$  specified above. As expected, a much higher degree of modulation in the density profile is present for the strongly diffracting grating. For the weakly diffracting grating of Fig. 1(a) and 2(a), a far milder variation in adsorbate density is seen. The peak adsorbate density in Fig. 4 is set equal to that of the homogeneous film before the grating formation. This value agrees, within experimental accuracy, with a calibration of the strength of the diffracted SH beams based on the the SH reflection from the un-modulated adsorbed monolayer.

We now treat briefly a model for the formation of the molecular grating. The gratings are formed by exposing the molecular films to intense radiation at a wavelength of 532 nm. This wavelength lies in a region of strong absorption associated with the  $S_1 \leftarrow S_0$  transition in the dye molecules, suggesting that a thermal desorption process may be operative.<sup>10</sup> A thermal desorption mechanism is supported by the results of grating formation for molecules adsorbed on sapphire, rather than fused silica substrates. Under similar conditions of exposure, as shown in Fig. 3, a much weaker grating is formed for adsorbed molecules on the sapphire substrate. If the adsorbate/substrate interaction is comparable in the two cases, then this behavior is a natural consequence of the differing thermal properties of the two substrates. The much higher thermal conductivity of sapphire compared with fused silica implies a far smaller temperature rise for the same rate of energy deposition.

Here we apply the thermal desorption model to the grating formation on the fused silica substrates. The results of this analysis can then be compared with the adsorbate density profiles inferred from the SH diffraction measurements. The temperature at the surface of the sample is computed by solving the thermal diffusion equation<sup>11</sup> with

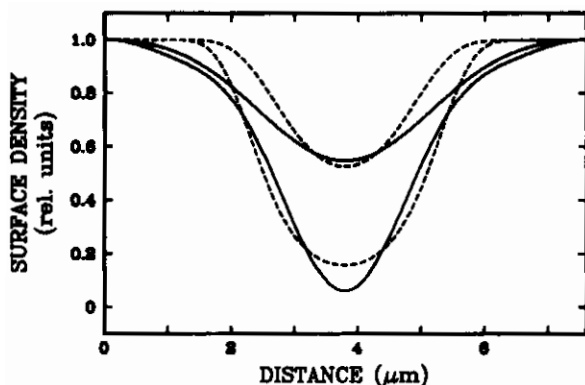


Fig. 4. Average surface densities for the monolayer gratings compared to the original densities of the homogeneous monolayers as a function of spatial position. The solid curves are based on the experimental diffraction patterns and the dotted curves are obtained from the thermal desorption model discussed in the text. The weakly modulated grating was formed with a desorption fluence of  $1.1 \text{ J/cm}^2$  and the strongly modulated grating with  $1.6 \text{ J/cm}^2$ , corresponding, respectively, to the upper and lower panels in Figs. 1 and 2.

values for the heat capacity and the thermal conductivity taken from the literature and approximated as temperature independent. The rate of heat deposition in the surface layer is determined from the temporal profile of the laser intensity and the measured linear absorption of the molecular film. Heat deposition in the bulk of the substrate is assumed to be negligible. Since the thermal diffusion length in fused silica is far less than the grating spacing for the nanosecond desorption pulses employed in these measurements, we can treat the thermal diffusion equation as one dimensional. The peak temperature along the surface is then found to be given by

$$[7] \quad T_s(x,y) = T_o + \alpha F \xi (4/\pi t_p C K)^{1/2} (1 + \cos \mathbf{k}_g \cdot \mathbf{x}) .$$

In this relation,  $C$ ,  $K$  and  $T_o$  refer, respectively, to the heat capacity (per unit volume), the thermal conductivity, and the initial temperature of the substrate;  $\alpha$  represents the absorption coefficient of the adsorbed layer; and  $F$  is the fluence of the desorbing radiation averaged across surface. The time  $t_p$  is a measure of the laser pulse duration and  $\xi$  is a numerical coefficient of order unity reflecting the temporal profile of the laser pulse. (For a pulse with uniform intensity in time and duration  $t_p$ ,  $\xi = 1$ ; in the calculation, we have integrated numerically the experimental pulse shape to determine the coefficient  $\xi$ .) In Eq. [7], the laser intensity profile is taken to be that of an idealized interference pattern with wave vector  $\mathbf{k}_g$  resulting from two beams of equal intensities.

The thermal desorption mechanism is described by first-order kinetics with a pre-exponential factor  $\nu$  and an activation energy  $E_a$ . Treating these parameters as independent of adsorbate coverage, we obtain a simple expression for the adsorbate density across the surface after the grating has been formed by exposure to the laser radiation:

$$[8] \quad N_s(x,y) = N_{s,o} \exp\{ - \nu \tau \times \exp[ - E_a/k_B T_s(x,y) ] \} .$$

In obtaining this analytic form, we have taken the desorption rate to be negligible except for a time  $\tau \sim t_p$  while the surface is near its peak temperature  $T_s(x,y)$ .

The thermal desorption model for the formation of the grating outlined above has two adjustable parameters,  $\nu$  and  $E_a$ , characterizing the interaction of the adsorbed molecules with the substrate. We have chosen these parameters by fitting the strongly modulated density profile in Fig. 4. The result, indicated by the dashed line in Fig. 4, gives reasonable agreement considering the simplicity of the analysis. The density profile for the weak grating is also reproduced adequately from the model with the established values for  $\nu$  and  $E_a$  and the measured desorption fluence. We have extended the treatment of desorption to include the possible influence of optical saturation in the layer of adsorbed dye molecules, which may occur in the presence of the intense desorbing laser field. The saturation effect is introduced by replacing the low-intensity absorption coefficient  $\alpha$  by

$$[9] \quad \alpha(I) = \alpha(0)/[1 + I/I_{sat}] .$$

When this expression is introduced into our analysis, the form of the predicted adsorbate density profile (Eq. [8]) remains the same.<sup>12</sup> The parameters  $\nu$  and  $E_a$ , however, no longer give the pre-exponential factor and the activation energy for desorption directly, but are more complex expressions involving the saturation intensity  $I_{\text{sat}}$  and the surface temperature. The lack of a good estimate for the saturation intensity<sup>13</sup> thus poses difficulties in the extraction of accurate values for the physically interesting pre-exponential factor and the desorption activation energy. An estimate of  $E_a \sim 1.5\text{eV}$  can be given for the activation energy, nonetheless, because this quantity has a relatively mild dependence on the assumptions about the saturation intensity. The pre-exponential factor is found to vary over a wide range from  $10^{10}\text{ sec}^{-1}$  to over  $10^{17}\text{ sec}^{-1}$  and cannot be determined from this treatment.

The discussion here illustrates how the adsorbate density profiles deduced from the SH diffraction measurements can be used to determine interesting properties of the molecule/ substrate interaction. For a case in which direct laser heating of the substrate is present, the complications of optical saturation encountered above will not be present and more precise information should be obtainable.

## 6. CONCLUSIONS

The surface-specific process of optical second-harmonic generation has been seen to give rise to strong diffraction into several orders from periodically modulated surfaces. In this work, we have reported results for a static molecular grating associated with density variations and have demonstrated how the SH diffraction pattern can be related to the adsorbate density profile. It should be stressed that SH diffraction is expected to be sensitive to a variety of other periodic modifications in the top atomic layers of a surface. Just as for the analogous measurements in bulk materials, this technique is particularly powerful when applied in a time-resolved fashion. The work of Zhu *et al.*<sup>5</sup> on surface diffusion of adsorbates makes this point forcefully. Pump-probe measurements on an ultrafast time scale are also possible and should permit novel studies of relaxation processes at surfaces and interfaces to be performed.

## REFERENCES

1. For an overview, see *Laser-Induced Dynamic Gratings*, edited by H. J. Eicher, D. Pohl, and P. Günter, Springer Ser. Opt. Sci. **50** (Springer, Berlin, 1986); H. J. Eichler, IEEE J. Quantum Electron. QE-22, 1194 (1986) and following papers.
2. H. Bergner, V. Brückner, and M. Supianek, IEEE J. Quantum Electron. QE-22, 1306 (1986) and references therein.
3. For recent reviews, see Y. R. Shen, Ann. Rev. Mater. Sci. **16**, 69 (1986); Y.R. Shen, in *Chemistry and Structure of Interfaces: New Laser and Optical Techniques*, edited by R.B. Hall and A.B. Ellis (Verlag Chemie, Weinheim, 1986), p. 151; G. I. Richmond, J. M. Robinson, and V. L. Shannon, Prog. in Surface Sci. **28**, 1 (1988).
4. G. A. Reider, M. Huemer, and A. J. Schmidt, Optics Commun. **68**, 149 (1988).
5. X. D. Zhu, Th. Rasing, and Y. R. Shen, Phys. Rev. Lett. **61**, 2883 (1988).
6. T. Suzuki and T. F. Heinz, submitted for publication
7. A. Wokaun *et al.*, Phys. Rev. **B24**, 849 (1981).
8. T. F. Heinz, C. K. Chen, D. Ricard, and Y. R. Shen, Phys. Rev. Lett. **48**, 478 (1982).
9. K. Kemnitz *et al.*, Chem. Phys. Lett. **131**, 285 (1986) and references therein.
10. A thermal mechanism for desorption of dye molecules in thin films irradiated by nanosecond laser pulses is presented in S. E. Egorov, V. S. Letokhov, and A. N. Shibanov, Kvantovaya Elektron. **11**, 1139 (1984) [ Sov. J. Quantum Electron. **14**, 940 (1984) ].
11. J. F. Ready, *Effects of High Power Laser Radiation*, (Academic Press, New York, 1971), Ch. 3.
12. It should be noted that this property holds when the spatial variation of the desorbing laser intensity is taken into account in describing optical saturation; the detailed temporal structure of the laser pulse should be less significant in determining the adsorbate density profile and is omitted from consideration here.
13. A high saturation intensity is suggested by the sub-nanosecond fluorescence lifetime of adsorbed dye molecules. See K. Kemnitz, N. Tamai, I. Yamazaki, N. Nakashima, and K. Yoshihara, J. Phys. Chem. **90**, 5094 (1986) and references therein.